Optimization of Quantum Dot Loading into Micelles and Purification for Biological Imaging

Autumn 2016

Submitted by: Christopher Chang

Faculty Advisor: Dr. Jessica O. Winter, William D. Lowrie Department of Chemical Engineering

Abstract

Personalized medicine to treat cancer, immunodeficiencies, and neurological disorders has expanded rapidly in the 21st century. However, diagnosis and treatment of these diseases at a molecular level is limited by current biological imaging techniques. Quantum dots have enormous potential as a biological imaging agent, with size-tunable and narrow emission spectra, improved stability over molecular dyes, and the potential for multiplexed imaging. Most quantum dots are synthesized via organic procedures that may be toxic and require either surface modification or encapsulation into nanocarriers, such as micelles. The assembly of polymers and quantum dots into micelle complexes has not been optimized. Additionally, purification of these nanoparticle complexes can be difficult. This work examines some of the factors that may influence quantum dot loading, as well purification, via chloroform liquid-liquid extraction. In the interfacial instability method, it is hypothesized that the quantum dot to polymer ratio has an effect on quantum dot loading. Additionally, the solvent used in solvent exchange is expected to alter the efficiency of quantum dot loading. No significance was found in either of these factors, likely due to an uncontrolled variation in experimental settings. Chloroform extraction is hypothesized to remove empty micelles and unencapsulated quantum dots from quantum dot micelle solutions. Through transmission electron microscopy, chloroform extraction is shown to be an effective technique to remove these impurities. Further work in optimization of quantum dot loading and purification techniques would create better quantum dot imaging labels for biological applications.

Acknowledgements

The author gratefully acknowledges The College of Engineering and The Undergraduate Research Office at The Ohio State University for the opportunity and the funding to conduct this research, and Dr. Jessica Winter for her mentorship and support throughout the duration of this project. Additionally, the author acknowledges Dr. Qirui Fan, Gauri Nabar, Abhilasha Dehankar, and the other members of the Winter Lab for their guidance and collaboration.

Table of Contents

List of Tables and Figures

Introduction

Since their inception, quantum dots (QDs) have shown potential as a fluorescent reporter for biological imaging applications.[1-3] QDs are semiconductor nanocrystals ranging from 1 to 10 nanometers. When excited by light, QDs exhibit quantum confinement leading to a number of unique size-dependent properties.[4-6] The unique properties of QDs offer significant advantages over current standard molecular dyes. These advantages include tunable light emission, a bright signal, resistance to photo-bleaching (Figure 1C), a broad range of excitation wavelengths, and a narrow emission spectrum.[1, 2, 4, 6-9] The narrow emission bandwidth allows for the potential to utilize QDs as a multimodal imaging agent (Figures 1A, 1B). That is, multiple QDs of varying colors may absorb light effectively over a wide range, and emit multiple, differentiable emission peaks within the visible spectrum.[5, 6, 8] The Stokes shift, or the wavelength distance between excitation and the QD emission wavelength, is generally large for quantum dots, allowing QDs to be a good candidate for imaging biological issue with high background autofluorescence.[6]

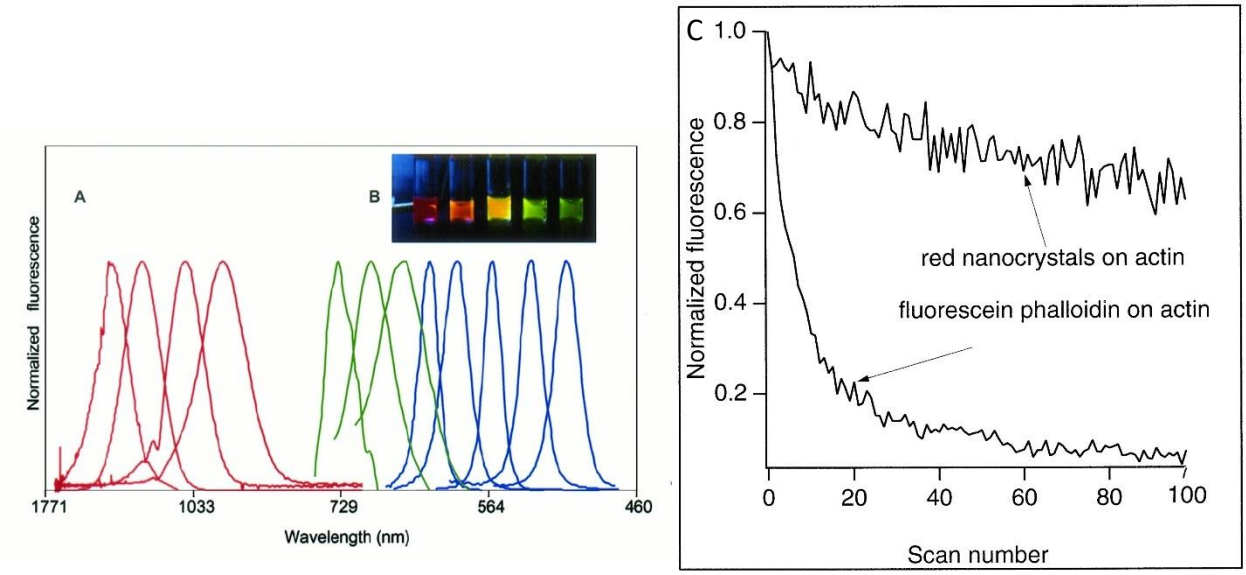

Figure 1: Advantages of QDs. (A) Multiple spectra fit into the same emission profile, (B) size-tunable QDs allow for tunable light emission, (C) resistance to photo-bleaching over time compared to molecular dyes.1

With multimodal capabilities, QDs have an exciting potential to be used as a diagnostic tool for cancer, immunodeficiencies, and neurological disorders.[5] Currently, diagnostic approaches utilize screening for genetic and phenotypic signatures of diseases cells, such as immunohistochemistry, Western blot, and ELISA. These diagnostic tools are limited by the number of biomarkers that can be simultaneously tracked and analyzed, lack of real time imaging of cellular processes, and may be based on qualitative judgements.[4, 5] Multiplexed, QD-based imaging of biomarkers can increase diagnostic sensitivity and specificity.[9] As medicine continues to advance towards personalized medicine, or the diagnosis and treatment of diseases from whole-body to molecular perspectives, there is a need for improvement upon current imaging and diagnostic practices. QDs address many of the current limitations with their ability to create multiplexed signals with size-tunable and narrow emission spectra, increased stability and increased brightness, and a large Stokes shift, which may lead to improved diagnoses, prognoses, and treatment outcomes.[5]

Most QDs are comprised of a metallic core (e.g. ZnS)/shell (e.g. CdSe) structure.[4] Additionally, due to synthesis conditions, hydrophobic organic ligands often coat the surface.[4, 8, 10] The composition of QDs presents an issue for biological applications; QDs are not water soluble. Cd in QDs is also toxic, and is recognized as a carcinogen. In order for QDs to become biologically suitable, they must be non-toxic and non-biologically active, and must be stable for a long period of time.[10] To address this, researchers have attempted to utilize a ligand exchange method to replace the organic ligands with more polar ligands, either as a monolayer and multilayer.[4, 8, 10] The monolayer approach produces QDs with poor colloidal stability, whereas the multilayered

coating of more polar ligands is difficult and inefficient. Additionally, both methods produce QDs that have a tendency to aggregate and physically absorb nonspecifically.[10]

In 2002, Dubertret et al. published a method of encapsulating individual QDs in phospholipid block-copolymers via thin film hydration, and showed that their nanoparticle tag could be used in *in vivo* and *in vitro* studies. These QD-micelle complexes can be seen below in Figure 2.[10]

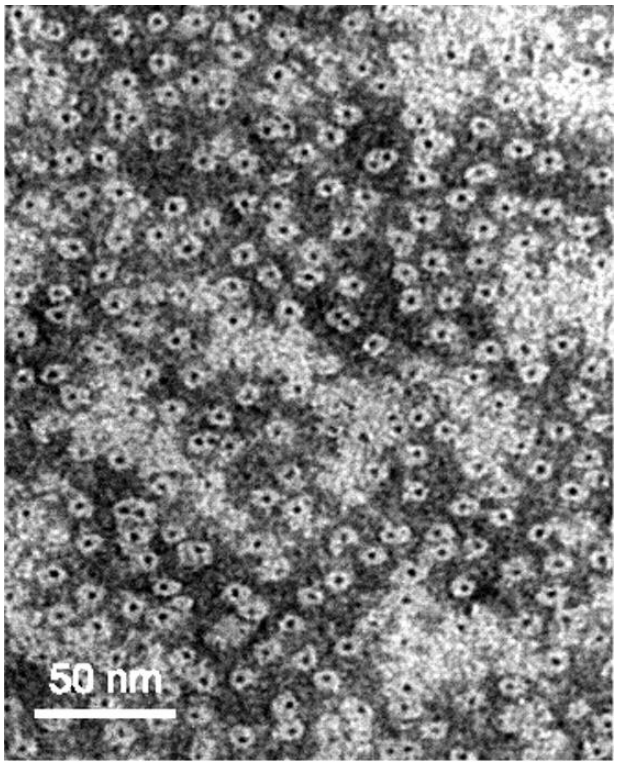

Figure 2: Single QDs encapsulated in phospholipid block-copolymers.[10]

This method addressed several of the issues with non-specific binding.[10] Thin film hydration encapsulates QDs in micelles so that they may be used in biological applications.[11] Another method of micelle self-assembly was described by Zhu and Hayward. This method takes advantage of interfacial instabilities of emulsion droplets to create micelles comprised of amphiphilic block-copolymers. The block-copolymers are dissolved in a water immiscible organic phase (chloroform) and mixed with an aqueous phase to form an emulsion. As the chloroform

diffuses and evaporates, the block-copolymers self-assemble into a micellar structure, and the surface area to volume ratio of the shrinking droplets increases. As the organic-aqueous interface becomes increasingly unstable, the micellar assemblies are ejected into the aqueous phase.[12] Self-assembly of micelles can be applied to encapsulate QDs and other nanoparticles.[4,7] This process encapsulates multiple QDs, referred to as Multidots.

Empirically, micelle encapsulation of QDs is not trivial. Loading QDs into micelles may be inefficient, leading to empty micelles or un-encapsulated quantum dots that precipitate out of solution. Micelles and QDs may also aggregate into globular structures, rendering them incompatible for biological use. Another challenge emerges in the purification of micelle encapsulated QDs from empty micelles, aggregates, and other impurities. This research aims to optimize procedures in order to increase the efficiency of QD loading into micelles, and the purification of these nanoparticles via liquid-liquid extraction(LLE) with chloroform.

Methodology

Materials

Methanol (≥99.8%), isopropanol (≥99.7%), toluene (≥99.8%), acetone (≥99.9%), ferric chloride, ammonium thiocyanate, and Poly (vinyl alcohol) (13000–23000 Dalton, 87–89% hydrolyzed, PVA) were purchased from SigmaAldrich. Chloroform was purchased from Mallinckrodt Chemicals. Poly(styrene-b-ethylene oxide) (PS-PEO) with a molecular weight of 9500-b-18000 (Dalton) was purchased from Polymer Source. 1,2-dipalmitoyl-*sn*-glycero-3-phosphoethanolamine-N-[methoxy(polyethylene glycol)-2000] (DSPE-PEG-2000) and 1,2-distearoyl-*sn*-glycero-3-phosphoethanolamine-N-[amino(polyethylene glycol)-2000] (DSPE-PEG-2000-NH2) werewas purchased from Avanti Polar Lipids Inc. CdSe core QDs (λ_{em}=540) were purchased from NN-Labs. ZnS-CdSe organic QDs in decane (λ_{em}=545) were purchased from Invitrogen.

Interfacial Instability Method

This protocol was modified from J.T. Zhu et al.[12] CdSe QDs (120 µl , λ_{em}=540, 10mg/mL in toluene) were solvent exchanged with 240 µL of a methanol-acetone mixture of varying ratios (1:4, 2:3, 1:1, and 4:1). The methanol-acetone mixture precipitated the QDs. The solution was then centrifuged at 7000 rcf for 30 seconds, and the supernatant was removed. Varying amounts of PS-PEO (6.6 mg, 24.01 mg, 40 mg, and 240.1 mg) were dissolved in 330 µL chloroform and mixed into the QD precipitate to vary the QD:PS-PEO ratio up to 1:100. PVA was prepared as a 5 wt% concentration and warmed to 30°C. The QD mixture was added to 9 mL PVA and mixed briefly to create an emulsion. The solution was then low-mode bath sonicated for 15 minutes at 30°C. At 1, 2, 4, 8, and 12 minutes, the solution was removed and vortexed for 5 seconds and then

returned to the sonication bath. After 15 minutes, the QD/PVA solution emulsion was added to an aluminum dish and placed on a rocker until the solution turned transparent. The solution was then collected and centrifuged at 1000 rcf for 30 seconds to precipitate any large aggregates, and then stored at 4°C.

Thin Film Hydration Method

This protocol was modified from Dubertret et al.[10] Isopropanol and methanol were mixed at a ratio of 1:2. QDs (450µL, λ_{em}=545, 1 µM) in decane were added and mixed briefly. The solution was centrifuged at 1000 rcf for 4 minutes. The supernatant was removed, and the precipitate was allowed to dry for 3.5 hours. Chloroform (100 µL) was then added to dissolve the dried precipitate. The lipid solution was prepared as either DSPE-PEG-2000 (20 mg/mL) in chloroform or DSPE-PEG-2000:DSPE-PEG-2000-NH2 = 9:1 (20 mg/mL) in chloroform. The lipid solution (5 µL) was mixed with the QD solution and allowed to incubate and dry for 3 hours. The solution was then dried under vacuum for an additional 1 hour. The thin film was then heated to 80°C for 30 seconds in a water bath; then 60µL of deionized water (80°C) was added. The solution was mixed for 1 minute to yield QDs encapsulated in micelles. The solution was stored at 4°C. TEM was conducted within 24 hours.

Chloroform extraction of empty micelles

QDs encapsulated into micelles composed of DSPE-PEG-2000 were subjected to liquid-liquid extraction (LLE). Chloroform was added to samples of QD micelles and mixed for varying amounts of time. The chloroform was then removed for absorbance analysis and TEM imaging.

Characterization of micelle encapsulated QDs

Transmission electron microscopy (TEM) was performed using an FEI Tecnai G2 Spirit TEM. Prior to imaging, samples were negatively stained with 1% uranyl acetate to identify micelles. Fluorescence emission spectra were measured using a PTI QuantaMaster™ 40. Absorbance spectra were collected with a Thermo Electron Corporation Genesys 6 spectrophotometer.

Quantification of empty micelle removal

This protocol was adopted from J.C.M. Stewart.[13] Ferric chloride (27 g) and 30 g ammonium thiocyanate (NH_4SCN) were dissolved in 1 L water to form a working solution. To create a calibration curve, DSPE-PEG-2000 was dissolved in chloroform to yield concentrations of 3.125, 6.25, 12.5, 21.875, and 31.25 µg/mL. To test a sample of interest, 100 µL water, 100 µL working solution and 400 µL DSPE-PEG chloroform solution were mixed for 1 minute and centrifuged at 3000 rpm for 1 minute. The supernatant was extracted and its absorbance was measured at 488 nm. Beer's law was used to analyze the absorbance to obtain concentration.

Results and Discussion

Optimization of Multidot Loading

Multidots were assembled via interfacial stability by emulsifying the solution with 9 mL PVA solution (5 wt%). To examine factors that may influence the efficiency of micelle loading, the ratio of QD to polymer was examined. The polymer solution was mixed with the QD solution in a molar ratio between 0.01 and 0.1 gmol PS-PEO/gmol QD. For the control, 6.6 mg PS-PEO was used, as stated in the standard operating procedure.

The ratio of methanol to acetone used for solvent exchange was also examined. Solvent exchange into a solution of methanol and acetone from toluene allowed the QDs to precipitate and exchange with chloroform. Ratios of methanol to acetone (1:4, 2:3, 4:1) were mixed to obtain an intermediate solvent that could transition the exchange from toluene to chloroform. The control used a methanol-acetone mixture in a 2:3 ratio, or 96 µL methanol to 144 µL acetone.

Fluorescence was measured as a surrogate variable to quantify QD loading. The maximum fluorescence intensity as a response is reported in Table 1 below.

Table 1: Fluorescence intensity as a response to mass of polymer added and methanol volume used for solvent exchange

Mass Polymer (mg)	Volume methanol (uL)	Fluorescence intensity
6.6	48	181017
6.6	48	177517
6.6	48	118877
6.6	96	136141
6.6	96	162356
6.6	96	138146
12.2	96	228870
12.2	96	111453
12.2	96	91228

An analysis of variance (ANOVA) found a p-value of 0.4866. There was not enough evidence to suggest that mass of polymer added and volume of methanol used in solvent exchange have any effect on the fluorescence intensity of the Multidots. Parameter tests yielded p-values of 0.7134 and 0.9631, respectively.

TEM images were also taken to characterized the Multidots. Figure 3 below and Figure 7 in the appendix show the TEM images of the control group with the PS-PEO mass and methanol volume suggested in the standard protocol. Figure 4 below and Figures 8 and 9 in the Appendix depict the TEM images of the experimental groups.

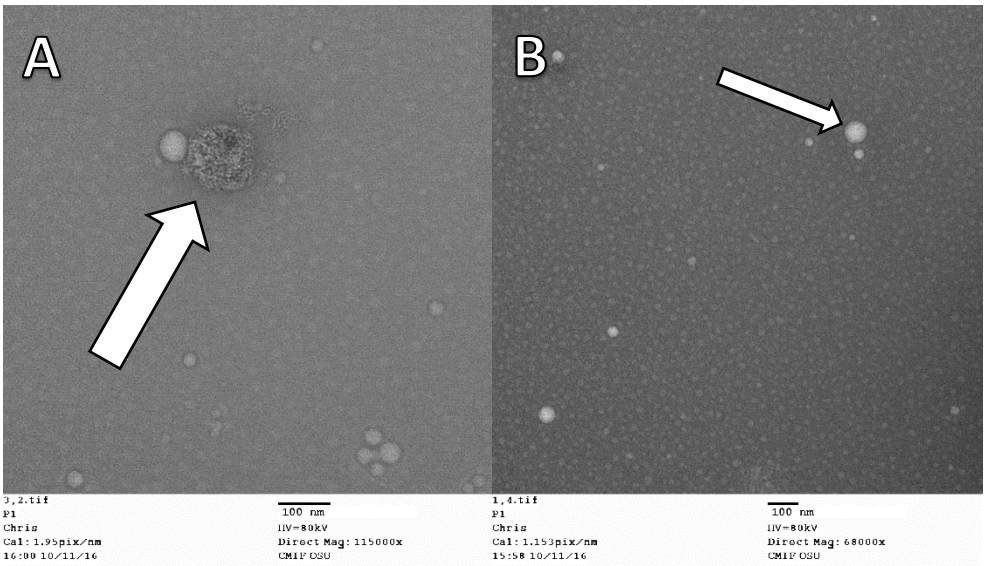

Figure 3: TEM images of control group (6.6 mg PS-PEO addition, 96 µL methanol added during solvent exchange). (A) An aggregate of QDs encapsulated by PS-PEO, (B) empty micelles

TEM images were omitted for experimental samples other than 24.01 mg PS-PEO and 192 µL methanol and 240.1 mg PS-PEO and 48 µL methanol due to the fact that the negative stain was too dark to produce any usable pictures.

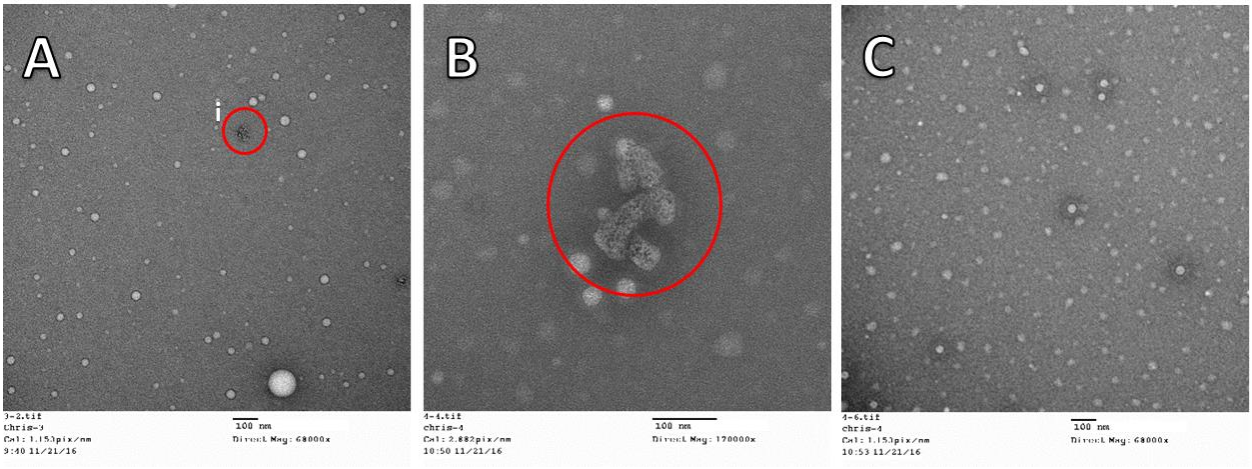

Figure 4: TEM images of Multidot micelles with experimental factors. (A) Empty micelles in sample with 24.01 mg PS-PEO and 192 µL methanol. (i) Aggregate of unencapsulated QDs, (B) large QD + micelle aggregation in sample with 240.1 mg PS-PEO and 48 µL methanol, (C) empty micelles in 240.1 mg PS-PEO and 48 µL methanol sample.

In each of the samples imaged, there were a significant number of empty micelles, with little to no encapsulated QDs. Figures 4A and 4C show empty micelles scattered on the grid. In Figure 4A(i), there are groupings of aggregated QDs that have not been encapsulated. Figure 4B above shows an aggregate of QDs that have been encapsulated by PS-PEO. These results suggest that the efficiency of micelle loading is still low, even for control groups. Upon examination of the bulk solution, the QDs remain fluorescent, suggesting that the TEM images are not representative of the solution. Larger QD aggregates may have dispensed at the bottom of the solution and not been sampled.

The results seen in the TEM suggest that the protocol has not been optimized for QD loading. The control, which followed the protocol, did not yield many encapsulated QDs. Additionally, the changes to amount of PS-PEO added and the volume of methanol used in the solvent exchange did not seem to increase QD loading. Not all the samples could be imaged, but with a non-significant p-value in analysis of the effect of polymer mass and volume of methanol on fluorescence intensity, it suggests that the amount of PS-PEO and the volume of methanol do not have significant effects on quantum dot loading.

Quantum Dot Purification

Known concentrations of DSPE-PEG dissolved in chloroform were used to create a calibration curve between absorbance spectra and concentration. Lipid solutions of 3.125, 6.25, 12.5, 21.875, and 31.25 µg/mL DPSE-PEG in chloroform had their absorbance measured. Beer's law relating absorbance of a material to its concentration was used to analyze this data and generate a calibration curve. The calibration curve can be seen below in Figure 5. The absorbance at 31.25 µg/mL DPSE-PEG in chloroform was omitted from the trend line since it extended beyond the linear range. This calibration curve may be used to relate light absorption from DSPE-PEG removed in chloroform to quantify the about of lipid removed.

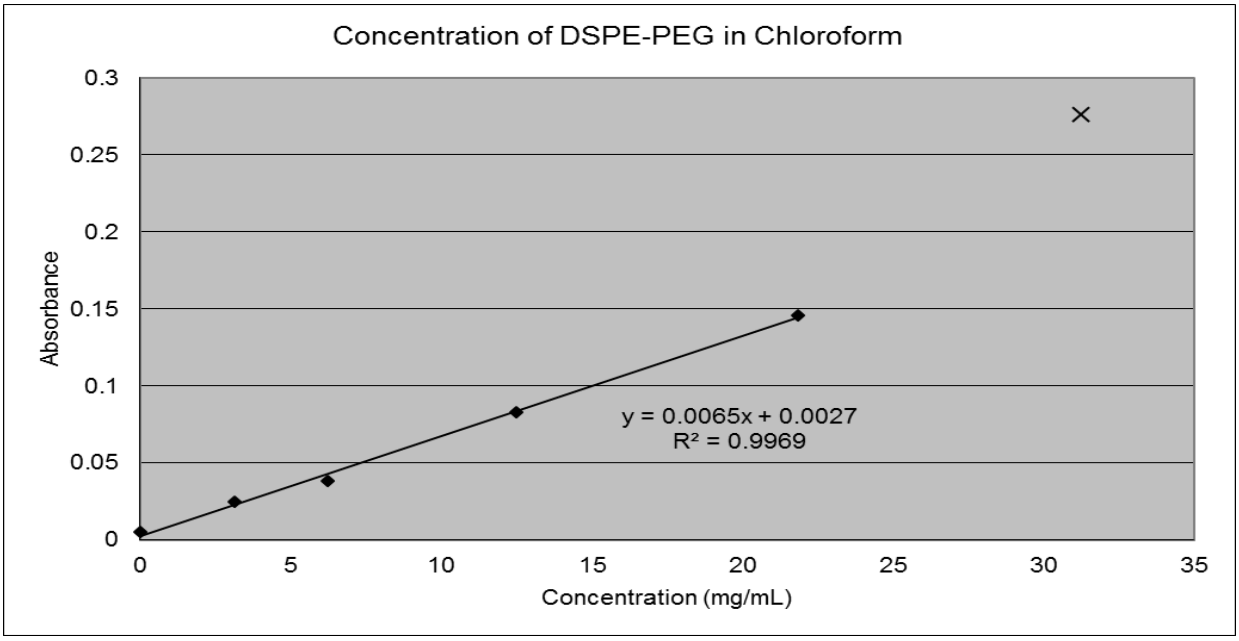

Figure 5: Calibration curve determining concentration of DSPE-PEG dissolved in chloroform based on absorbance. "X" depicts the point removed from the trendline fit, since it extends beyond the linear range.

TEM imaging was conducted on a sample of single QDs encapsulated in DSPE-PEG micelles before and after chloroform LLE. These images can be seen below in Figure 6. Before chloroform extraction (Figure 6A), approximately 43% of the nanoparticles are empty micelles, 16% are

unencapsulated QDs, and 41% are individual QDs encapsulated in DSPE-PEG micelles. After chloroform extraction (Figure 6B), approximately 1% of the nanoparticles are empty micelles, and 99% are the desired QDs encapsulated in DSPE-PEG micelles. No unencapsulated QDs can be seen after chloroform LLE. The number of empty micelles is reduced after chloroform extraction, suggesting that chloroform LLE may be an effective method of removing empty micelles and unencapsulated QDs through purifying the aqueous QD solution.

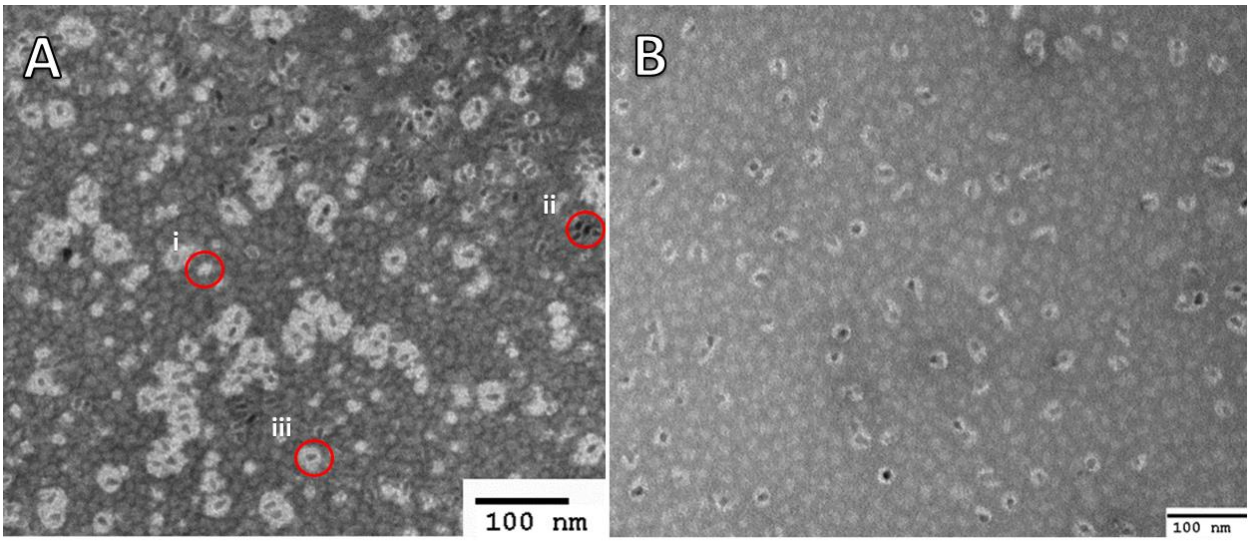

Figure 6: TEM images of QDs encapsulated in DSPE-PEG micelles. (A) Before chloroform LLE (i) empty micelle, (ii) unencapsulated QDs, (iii) QD encapsulated in DSPE-PEG. (B) After chloroform LLE.

It is worthwhile to note that the appearance of QD solution changed during chloroform LLE. Prior to mixing, the solution appeared transparent. After mixing, the solution appeared turbid. While chloroform mixed with water generally forms a cloudy appearance, if the chloroform extraction interacted with the surface ligands of the QDs it may have altered their optical properties. More studies would need to be conducted to determine whether or not the stability or optical properties of the QDs changed as a result of chloroform LLE, or if impurities were introduced into the solution.

Conclusion

This study aimed to determine factors significant to the optimization of QD assembly into micelles, and a potential method for purifying empty micelles from desired QD complexes. Using an interfacial instability route,[4,12] a two-parameter screening experiment was conducted. First, the QD to polymer ratio was studied, ranging from 1:10 to 1:100. Then the ratio of methanol to acetone was also examined, with ratios of 1:4, 2:3, 4:1.

Quantum dot loading for the experimental groups and the control group proved to be largely unsuccessful. QD loading as a response to changing QD:polymer ratio and composition of the solvent used in solvent exchange was measured using fluorescence. No significance was found in either of these factors (whole model p-value=0.4866).

QDs did not appear in most of the TEM images. Most images showed a large quantity of empty micelles. Large aggregates of QDs encapsulated by PS-PEO were captured, suggesting that QDs may have formed these larger structures during self-assembly, that had not been sampled when extracted for TEM imaging. The larger density of these particles may have moved to the bottom of the solution.

QD:polymer ratio and volume of methanol used in solvent exchange were not found to be significant factors in increasing QD loading, they should not be left out from future analysis. Their effects may be overshadowed by interaction with effects not studied in this work. Emulsification, sonication, and rate of organic evaporation in the interfacial instability route likely have a significant impact on QD loading. Due to limitations in the experimental lab space, these variables could not be well controlled. For future work, the introduction of QDs and polymer in

an organic phase to an aqueous PVA solution could be better regulated. Controlled injection of the organic phase with a jet or spray may provide a uniform method of dispersing the organic phase into the aqueous. Bath sonication was used to introduce energy to the system to disrupt the organic-aqueous interface. Other studies have attempted to use probe sonication.[4] A comparison of these methods based on the working volume of QDs may be a worthwhile investigation. Finally, the rate at which the organic phase evaporated could not be well controlled. The time scale of this evaporation took place between 3 and 8 hours. Controlling the evaporation using an isobaric process may provide a more controlled approach to organic solvent evaporation.

R. J. Hickey et al. reports that solvent-nanoparticle and polymer-nanoparticle interactions have significant effects on the assembly of nanoparticles and block-copolymers into micelles.[14] The solvent itself and the size of the hydrophobic and hydrophilic blocks on the polymer could be studied to optimize this system in the future.

In addition to solvent identity and polymer properties, a co-solvent technique exists for the encapsulation of QDs into micelles.[11,14] Quantitative comparisons of co-solvent, thin film hydration, and interfacial instability techniques should be examined. Throughput of these techniques is another concern. Co-solvent, thin film hydration, and interfacial instability methods are small batch, bottom up processes. Electrospray technology may provide a way to encapsulate micelles via a top down, high throughput process.[15]

The chloroform extraction provided initially promising results. The TEM images show a decrease in the number of empty micelles found after chloroform LLE. This method could potentially be

expanded towards other micelle systems in need of purification. A reduction in the number of empty micelles contaminating a solution of micelle encapsulated QDs would increase the effectiveness of QD probes as a biological imaging agent. In addition to testing this LLE technique on other micelle systems, the stability and optical properties of the purified QD solutions should be compared with non-purified solutions to ensure that the chloroform LLE does not adversely alter QD performance. Micelle degradation over time, degradation in response to photo-bleaching, and properties such as quantum yield should be investigated in future work.

Other separation methods could also be explored to purify QD-micelle complexes. Ultracentrifugation and size-exclusion chromatography may take advantage of the difference in densities between loaded micelles and empty micelles. Aggregated QDs also may be removed in these processes.

Once QD loading and purification have been optimized, the next aim would be to functionalize the QD complexes with antibodies for targeting of biomolecules. Currently, the chemistry to conjugate micelles to antibodies is inefficient. Introduction of antibodies into the complex also introduces potential unwanted contaminants, such as unconjugated micelles and antibodies.

Optimization of QD loading and purification is crucial to the future of these materials. QD imaging tags have incredible benefits to biological imaging of biomolecular processes, and may immensely improve diagnostic techniques of many prevalent diseases, including cancer, immunodeficiencies, and neurological disorders. In addition, the use of QDs would revolutionize the level of precision and resolution used to study physiological mechanisms at the molecular level.

Appendix

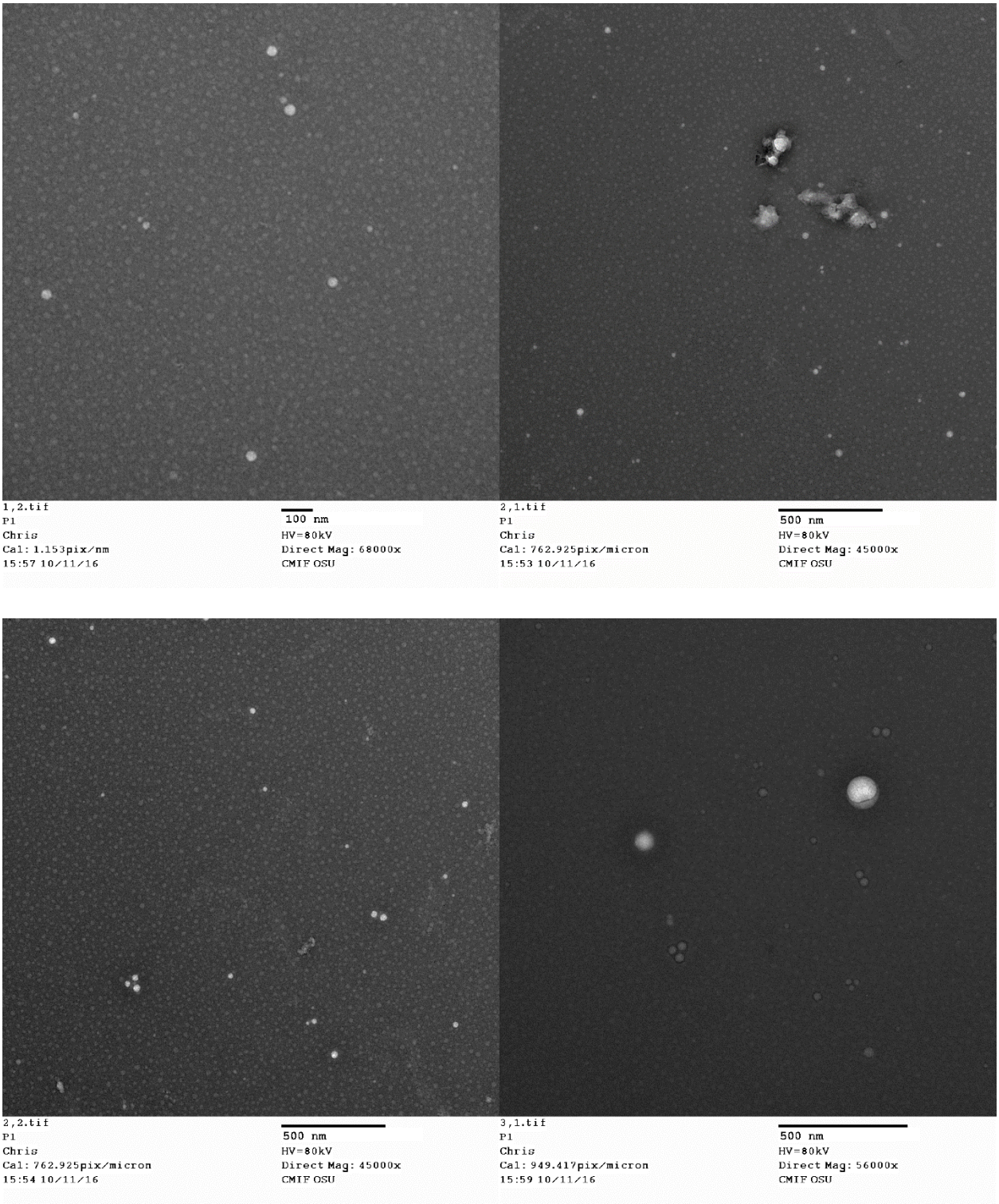

Figure 7: TEM images of control Multidots after assembly using standard protocol (6.6 mg PS-PEO addition, 96 µL methanol added during solvent exchange).

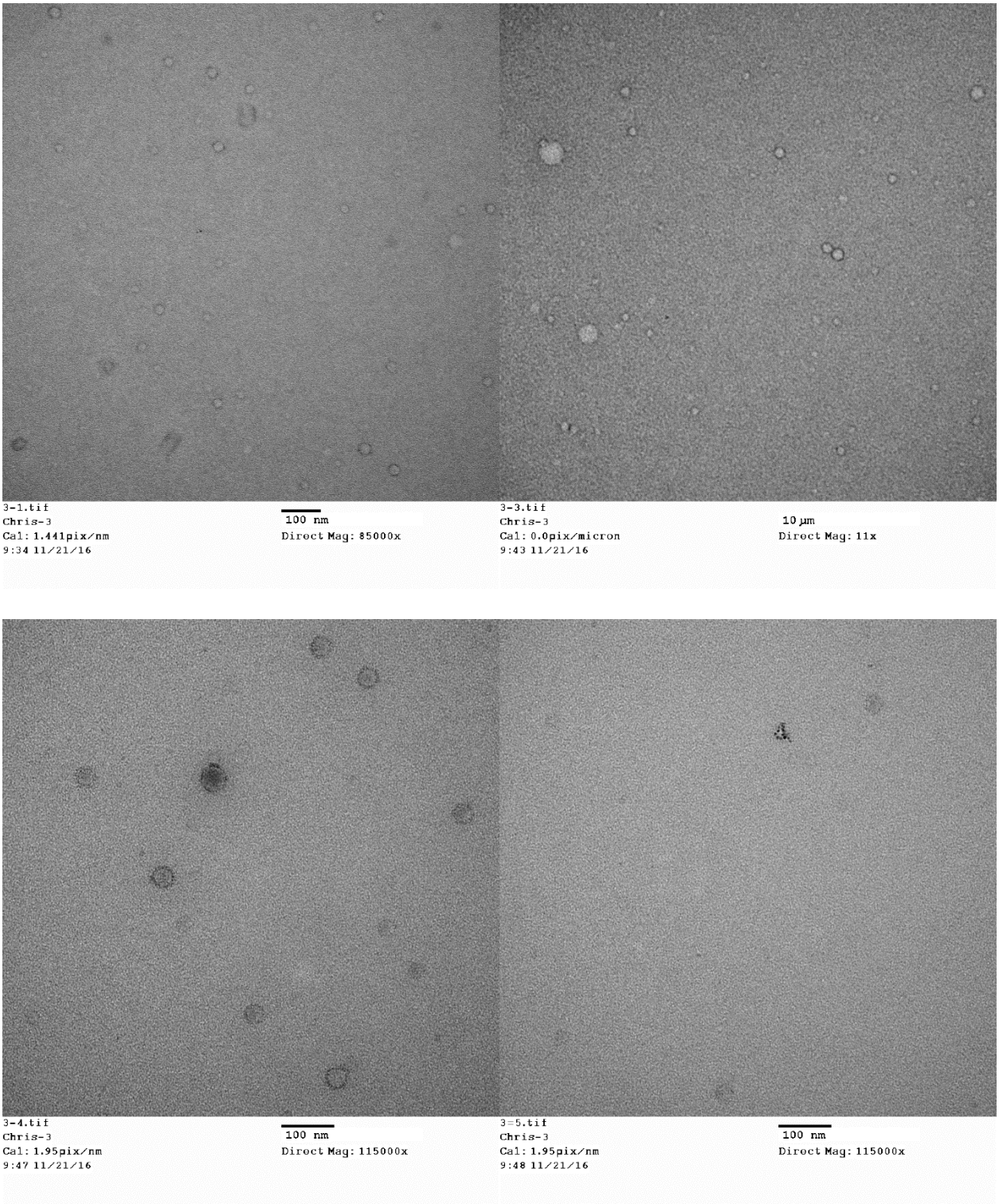

Figure 8: TEM images of Multidots (24.01 mg PS-PEO addition, 192 µL methanol added during solvent exchange)

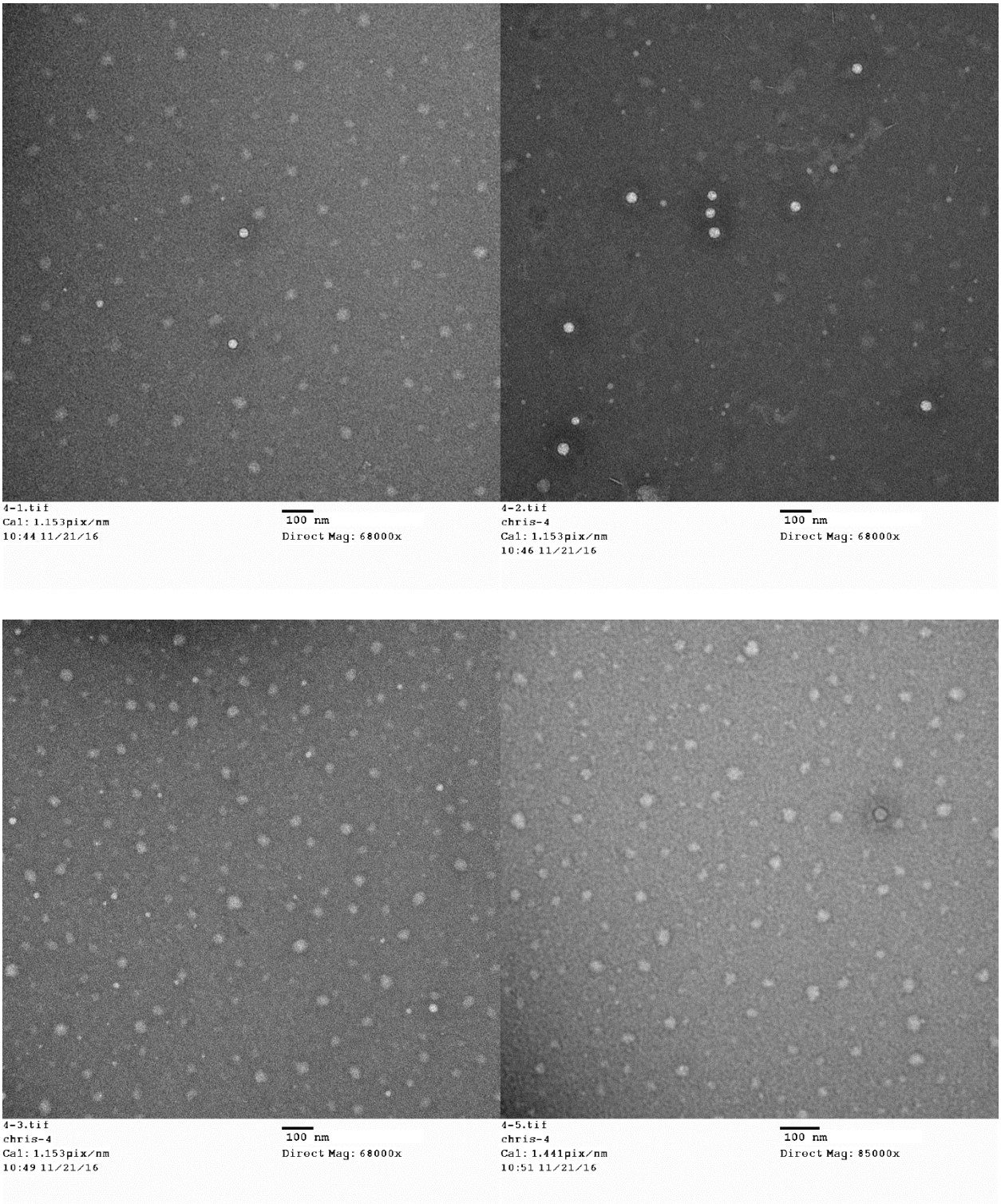

Figure 9: TEM images of Multidots (240.1 mg PS-PEO addition, 48 µL methanol added during solvent exchange)

References

1. Bruchez, M.; Moronne, M.; Gin, P.; Weiss, S.; Alivisatos, A. P., Semiconductor nanocrystals as fluorescent biological labels. *Science* **1998,** *281* (5385), 2013-2016.
2. Chan, W. C. W.; Nie, S. M., Quantum dot bioconjugates for ultrasensitive nonisotopic detection. *Science* **1998,** *281* (5385), 2016-2018.
3. Xu, J. Q.; Fan, Q. R.; Mahajan, K. D.; Ruan, G.; Herrington, A.; Tehrani, K. F.; Kner, P.; Winter, J. O., Micelle-templated composite quantum dots for super-resolution imaging. *Nanotechnology* **2014,** *25* (19), 11.
4. Mahajan, K. D.; Fan, Q. R.; Dorcena, J.; Ruan, G.; Winter, J. O., Magnetic quantum dots in biotechnology - synthesis and applications. *Biotechnology Journal* **2013,** *8* (12), 1424-1434.
5. Zrazhevskiy, P.; Gao, X. H., Multifunctional quantum dots for personalized medicine. *Nano Today* **2009,** *4* (5), 414-428.
6. True, L. D.; Gao, X. H., Quantum dots for molecular pathology - Their time has arrived. *Journal of Molecular Diagnostics* **2007,** *9* (1), 7-11.
7. Ruan, G.; Thakur, D.; Hawkins, S.; Winter, J. O. In *Synthesis and manipulation of multifunctional, fluorescent-magnetic nanoparticles for single molecule tracking*, Conference on Colloidal Quantum Dots for Biomedical Applications V, San Francisco, CA, Jan 23-25; Spie-Int Soc Optical Engineering: San Francisco, CA, 2010.
8. Kairdolf, B. A.; Smith, A. M.; Stokes, T. H.; Wang, M. D.; Young, A. N.; Nie, S. M., Semiconductor Quantum Dots for Bioimaging and Biodiagnostic Applications. In *Annual Review of Analytical Chemistry, Vol 6*, Cooks, R. G.; Pemberton, J. E., Eds. Annual Reviews: Palo Alto, 2013; Vol. 6, pp 143-162.
9. Liu, J. A.; Lau, S. K.; Varma, V. A.; Kairdolf, B. A.; Nie, S. M., Multiplexed Detection and Characterization of Rare Tumor Cells in Hodgkin's Lymphoma with Multicolor Quantum Dots. *Analytical Chemistry* **2010,** *82* (14), 6237-6243.
10. Dubertret, B.; Skourides, P.; Norris, D. J.; Noireaux, V.; Brivanlou, A. H.; Libchaber, A., In vivo imaging of quantum dots encapsulated in phospholipid micelles. *Science* **2002,** *298* (5599), 1759-1762.
11. Nabar, G.; Winter, J. O., Block-Copolymer Nanocomposites for Biomedical Applications. *Chemical Engineering Progress* **2014,** *110* (11), 51-54.
12. Zhu, J.; Hayward, R. C., Spontaneous generation of amphiphilic block copolymer micelles with multiple morphologies through interfacial instabilities. *Journal of the American Chemical Society* **2008,** *130* (23), 7496-7502.
13. Stewart, J. C. M., COLORIMETRIC DETERMINATION OF PHOSPHOLIPIDS WITH AMMONIUM FERROTHIOCYANATE. *Analytical Biochemistry* **1980,** *104* (1), 10-14.
14. Hickey, R. J.; Haynes, A. S.; Kikkawa, J. M.; Park, S.-J., Controlling the Self-Assembly Structure of Magnetic Nanoparticles and Amphiphilic Block-Copolymers: From Micelles to Vesicles. *Journal of the American Chemical Society* **2011,** *133* (5), 1517-1525.
15. Duong, A. D.; Ruan, G.; Mahajan, K.; Winter, J. O.; Wyslouzil, B. E., Scalable, Semicontinuous Production of Micelles Encapsulating Nanoparticles via Electrospray. *Langmuir* **2014,** *30* (14), 3939-3948.